J. Plant Biol. (2010) 53:121–133
DOI 10.1007/s12374-009-9095-x

ORIGINAL RESEARCH

Abnormal Vacuolization of the Tapetum During the Tetrad Stage is Associated with Male Sterility in the Recessive Genic Male Sterile *Brassica napus* L. Line 9012A

Lili Wan · Xiuyun Xia · Dengfeng Hong · Ji Li · Guangsheng Yang

Received: 21 November 2009 / Revised: 13 December 2009 / Accepted: 22 December 2009 / Published online: 2 February 2010

Abstract In the recessive genic male sterile line 9012A of *Brassica napus*, pollen development is affected during the tetrad stage. According to the light and electron microscopy analysis of tapetal cells and tetrads, the sterile tapetal cells swelled with expanded vacuoles at the early tetrad stage and finally filled the center of the locules where a majority of tetrads encased with the thick callose wall collapsed and degraded. We suggested that an absence of callase, which is a wall-degrading enzyme stored in the vacuoles of tapetal cells before secretion, resulted in the failure of tetrad separation. Moreover, transmission electron microscopy analysis showed that the secretory tapetal cells were not observed in sterile anthers, which indicated that the transition of the tapetum from the parietal type to the secretory type was probably aberrant. In plants, degeneration of the tapetum is thought to be the result of programmed cell death (PCD). PCD of tapetal cells was investigated by terminal deoxynucleotidyl transferase-mediated dUTP nick-end labeling assay and signals indicative of deoxyribonucleic acid fragmentation were detected much earlier in sterile anther than in fertile anther. This suggests that tapetal breakdown does not occur by the normal procession of PCD and might be following an alternative mechanism of unscheduled apoptosis in line 9012A. This research supports the hypothesis that premature PCD is associated with male sterility in *B. napus*.

L. Wan · X. Xia · D. Hong · J. Li · G. Yang (✉)
National Key Laboratory of Crop Genetic Improvement,
Huazhong Agricultural University,
Wuhan City, Hubei Province, China
e-mail: gsyang@mail.hzau.edu.cn

L. Wan
e-mail: wanlili122@yahoo.com.cn

Keywords Tapetum · Tetrad stage · Vacuole · Male sterility · Programmed cell death

Introduction

Most of higher plant species are hermaphroditic and male sterility is often considered as an accident of development. Among the multiple possible causes of male sterility, the most frequently met in nature is cytoplasmic male sterility (CMS), which is usually defined as "maternally" inherited deficiency in producing viable pollen, and the mitochondria are responsible for this trait (Budar and Pelletier 2001). Many genetic studies indicated that sexual processes are mainly controlled by alleles of nuclear genes designated as "ms" that affect male reproduction. These alleles are usually recessive, but a few of them are dominant (Ms) and both are typically expressed in specific sporophytic tissues at different stages (Horner and Palmer 1995). Gene mutation, interspecific and intraspecific hybridization, radiation, and genetic engineering can alter these genes, causing them either not to be expressed or to be expressed in an abnormal way, leading to sterility that regarded as "genic male sterility" (GMS).

According to a phenotypic scheme based on the level of expression, Kaul (1988) classified the natural and induced "GMS" into three categories: sporogenous, structural, and functional. Stamen development driven by sporogenous ms appears normal, but an abnormality occurs sometime between early microsporogenesis and late microgametogenesis, resulting in nonfunctional microspores or pollen. Structural ms is characterized by a pollenless anther or abnormally formed pollen and leads to the absence of microsporogenesis or its arrest sometime after inception (Johns et al. 1981). Functional ms is characterized by the

production of pollen but it is either not released from the anther or it is unable to reach the stigma to initiate fertilization (Horner and Palmer 1995). The application of GMS in rice, barely, wheat, soybean, cotton, and rapeseed, coupled with morphological and/or physiological traits, has met with success (Sorrells and Fritz 1982; Knapp and Cox 1988). Both recessive genic male sterility (RGMS) and dominant genic male sterility (DGMS) have been used in recurrent selection programs such to develop intermating populations that involve many parental lines and to synthesize populations for the improvement of one or several agronomic traits (Horner and Palmer 1995). Up to now, several GMS have been used in rapeseed hybrid production in China, such as a DGMS line (Li et al. 1990, 1995), three RGMS lines (Hou et al. 1990; Li et al. 1993; Tu et al. 1997), and a RGMS line with recessive suppressor gene (Chen et al. 1993, 1998; Ke et al. 2004). Especially, RGMS systems have another remarkable advantage that hybrids with strong heterosis are easily bred since most lines can be used as restores (He et al. 2008). The male sterility of 9012AB is controlled by two recessive genes (*Bnms3* and *Bnms4*) interacting with one recessive epistatic suppression gene (*Bnesp*; Chen et al. 1998; He et al. 2008). The genetic model indicates that a 100% sterile population (*Bnms3ms3ms4ms4Espesp*) can be obtained, with which a restorer line was used to cross to generate commercial F1 hybrid seeds. Although this kind of male sterility system have been increasingly used for rapeseed hybrid seeds production, cytological defects in 9012AB lines have not yet been carefully defined.

The differentiation of male gametes and pollen development involve an array of extraordinary events (Scott et al. 2004), which commences at the end of meiosis with the formation of a tetrad and ends at the dehiscence of anthers when the mature pollen grains are released. It relies on the orchestrated interaction and differentiation of both sporophytic and gametophytic tissues. As the innermost sporophytic cell layer that is in direct contact with microsporocytes, the tapetum is of considerable physiological significance because all the nutritional material entering the sporogenous cells/microspores/pollen grains passes through it or originates from it (Pacini et al. 1985). In addition, during certain periods of pollen development, it accumulates substantial quantities of reserve compounds (e.g., starch and protein crystals in plastids, lipid droplets and masses within and outside the plastids, soluble polysaccharides in the vacuoles; Pacini et al. 1985). In most species, including the Brassicaceae, the tapetum differentiation and subsequent disintegration coincides very well with the anther postmeiotic developmental program, and premature or delayed degradation will contribute to pollen abortion (Kawanabe et al. 2006; Li et al. 2006; Vizcay-Barrena and Wilson 2006). Sporogenous tissue (future gametophytic tissue) was completely surrounded by the tapetal layer. After the initial phase of cell expansion, cytoplasmic contact is lost between the microsporocytes and the tapetum, presumably by the synthesis of the microsporocyte callose wall. Following cytokinesis, the four haploid microspores produced from each microsporocyte are tetrahedrally arranged and termed a tetrad (Owen and Makaroff 1995). Tetrads in plants are typically enclosed in a thick wall composed of mostly callose (β-1,3-glucan) and other cell wall components such as cellulose and pectins (Rhee and Somerville 1998). It is believed that the callose layer is formed to prevent cell cohesion and fusion, and upon its degradation, it facilitates the release of free microspores into the locular space (Dong et al. 2005).

Similar to the secretion of many other molecules in plants, the enzymes responsible for the degradation of the tetrad wall are likely to be stored in certain subcellular compartments in the tapetal cells and secreted to the anther locule at the appropriate time. In soybean, the persistence of callose around the pollen mother cells (PMC) of *ms2* and *ms3* mutants is associated with the lack of secreted enzymes required for the dissolution of callose as well as rough endoplasmic reticulum (RER). Fei and Sawhney (1999) demonstrated that callose degradation by callase in *ms32* PMC was associated with the early formation of stacks of RER before meiosis in tapetal cells. Recently, complementary proteomic methodologies discovered the presence of β-1,3-glucanases and polygalacturonase within vegetative vacuoles, suggesting that vacuoles might be the ultimate storage site for at least two classes of tetrad wall-degrading enzymes. Of course, certain proteins containing signal peptides or transmembrane domains may be targeted to the vacuole via degradation or recycling processes (Wu and Yang 2005; Carter et al. 2004).

Hypertrophy of tapetal cells and their vacuolization towards the end of the tetrad stage, resulting in anther collapse, has been studied in *Arabidopsis* mutants. The tapetum and middle layer in *fat tapetum* mutant is much enlarged and the concurrent breakage and degeneration of microspores is also observed (Sanders et al. 1999). As in the *ms1* mutant, large autophagic vacuoles and abnormally swelling mitochondria were observed in the tapetum as well as within the microspore cytoplasm after the microspores are released from the tetrad (Ito and Shinozaki 2002; Wilson et al. 2001). In *myb33myb65* anthers, the tapetum underwent hypertrophy at the PMC stage, resulting in premeiotic abortion of pollen development (Millar and Gubler 2005). In the *Arabidopsis dyt1* mutant, the tapetal and middle layer cells swelled with expanded vacuoles and filled the center of the locules where the meiocytes had collapsed and degraded (Zhang et al. 2006). A mutation in the rice gene *OsUDT1*, which is a putative *DYT1* ortholog,

caused a failure of tapetal cell to differentiate and they became vacuolated during the meiotic stage. DAPI staining revealed that *udt-1* meiocytes underwent normal meiotic cell division and completely degenerated, leaving only their remnants at the center of the anther locules (Jung et al. 2005). A similar phenomenon was also observed in *Arabidopsis gus-negative1* (*gne1*) and *gne4* mutants where tapetal cells became highly vesicular and enlarged considerably from early prophase to late prophase and sporogenous cells were disrupted late in meiosis, surrounded by callose masses (Sorensen et al. 2002). These results suggest that tetrad wall-degrading enzymes might be synthesized in tapetal cells and stored in tapetal vacuoles prior to their secretion into the anther locule (Wu and Yang 2005).

In this report, a correlative structural approach using light and electron microscopy was employed to study anther development in RGMS (9012A) and fertile rapeseed plants (9012B). In addition, sterile anthers were studied in order to characterize defects in degenerated tetrads and/or abnormalities in the tapetum.

Material and Methods

Plants and Growth Conditions

The *Brassica napus* RGMS two-line, 9012AB, was provided by the National Center of Rapeseed Improvement in Wuhan. Plants were grown by sowing seeds in the rapeseed research field of Huazhong Agricultural University.

Light Microscopy

Buds were individually removed from inflorescences and fixed at room temperature for 24 h in ethanol 50% (*v*/*v*), acetic acid 5.0% (*v*/*v*), and formaldehyde 3.7% (*v*/*v*). After dehydration in an ethanol series, the samples were embedded in Technovit 7100 resin and sectioned (1 μm) using a fully motorized rotary microtome (Leica RM2265), then stained with 1% toluidine blue containing 0.1% sodium carbonate. Other samples were first stained with hematoxylin embedded in LR white resin and transversely sectioned into 6 μm slices using a microtome (Leica RM2235). Bright-field photographs of anther cross-sections were taken using a compound microscope.

Electron Microscopy

For transmission electron microscopy (TEM), stamens at various stages of development were prefixed in 2.5% glutaraldehyde adjusted to pH7.4 with 0.1 N sodium phosphate buffer and postfixed in 2% OsO_4 in the same buffer. Following an ethanol dehydration, samples were embedded in epoxy resin. Ultrathin sections (60 nm) obtained with a Leica UC6 ultramicrotome were double stained with 2% (*w*/*v*) uranyl acetate and 2.6% (*w*/*v*) lead citrate aqueous solution. Images were recorded using a Hitachi-7650 transmission electron microscope at 80 kV with a Gatan832 CCD camera (Wang et al. 1997). Scanning electron microscopy (SEM) observation was performed on anthers derived from fertile and sterile plants at the end of the tetrad stage. These samples were fixed overnight and dehydrated in a graded ethanol series as described for TEM, then dried to the critical point in liquid CO_2. Mounted samples were coated with palladium–gold in a sputter coater, then examined in a JSM-6390 scanning electron microscope.

Callose Staining and TUNEL Assay

For callose staining, flowers were fixed in ethanol/acetic acid (3:1, *v*/*v*) and stained with 0.01% aniline blue (Hong et al. 2001). Anther tissues were viewed on a fluorescent microscope using a UV filter. For the terminal deoxynucleotidyl transferase (TdT)-mediated dUTP nick-end labeling (TUNEL) assay, 6 μm sections were washed in phosphate-buffered saline (PBS; 160 mM NaCl, 2.7 mM KCl, 8 mM Na_2HPO_4, and 1.5 mM KH_2PO_4) for 5 min and incubated in 20 μg/ml proteinase K in 100 mM Tris–HCl (pH8.0) and 50 mM Na_2EDTA (100 μl per slide in a humidified chamber). The sections were washed in PBS for 5 min and fixed in 4% (*w*/*v*) paraformaldehyde in PBS for 10 min. In situ nick-end labeling of nuclear deoxyribonucleic acid (DNA) fragmentation was performed with a TUNEL apoptosis detection kit (DeadEnd™ Fluorometric TUNEL System, Promega) following the manufacturer's instructions. For each experiment, a positive control was prepared by treating the section with 1 U ul^{-1} DNaseI for 10 min at 37°C before labeling as above. The negative controls were labeled identically, except for the absence of the enzyme TdT. After the TUNEL reaction was stopped with 2X SSC and slides were rinsed with PBS (pH7.2), the slides were counter-stained with 1 μg ml^{-1} of propidium iodide (PI) for fluorescence. The fluorescent filter was set to view the green fluorescence of fluorescein at 520±20 nm, the red fluorescence of PI at >620 nm (Vizcay-Barrena and Wilson 2006).

Results

Cytological Analysis of the Events Leading to the Male Sterility in Recessive Genic Male Sterile *Brassica napus*

To examine anther morphological defects in the RGMS plant, anther sections were screened with a relative parallelism between bud size and the anther development. Anthers from buds <0.5 mm in length represented sporogenous mass stage.

Phase of premeiosis was observed in anthers from buds between 0.5 and 1 mm. Meiosis stage was indicated by the buds from 1 to 2 mm. Tetrads in the anther were mostly seen in 2–3 mm buds. Buds with 2.5–3.5 mm of length also contained developmental stages from the early microspore stage to vacuolated microspore stage. Bicellular and late/engorged pollen grains were obtained in anther locules from buds between 4 and 5.5 mm. The stages from early microspore to late pollen development were only observed in the fertile plants. Approximately 20 anthers from each stage were sectioned for both genotypes. Based on cellular events visible under the light microscope, we divided *B. napus* anther development into eight stages (Fig. 1). From the sporogenous mass stage to the early premeiosis stage both in fertile and sterile anthers, archesporial cells divided to form primary parietal cells that differentiated into the endothecium, middle layer, and tapetum, and primary sporogenous cells differentiated into the microsporocytes (Fig. 1a and f, b and g). Up to the microspore mother cell (MMC) stage, there were no obvious differences in anther cellular morphology including epidermis, endothecium, middle layer, tapetum, and microsporocytes found in either fertile or sterile anthers (Fig. 1c and h).

In fertile anthers, MMC underwent meiosis within each of the four locules and generated tetrads of haploid microspores. At this stage of development, sterile anthers exhibited detectable morphological abnormalities. Microsporocytes in sterile plants seemed normal and could undergo meiosis to form tetrads as observed in fertile anthers. However, the cytoplasm of tapetal cells was vacuolated compared with the agglomerate fertile tapetum (Figs. 1d and i and 2a, b). From the early microspore stage to vacuolated microspore stage in fertile anthers, microspores were released from tetrads and become vacuolated. In healthy anthers, the tapetal cells had deeply stained cytoplasm but no longer had large vacuoles (Fig. 1e and k). When each vacuolated microspore began to generate an exine wall and enter mitosis, the tapetum initiated degeneration (Fig. 1l). By the late pollen stage, the pollen grains (microgametophytes) consisting of two or three cells (one containing the tube nucleus; the others containing the generative nucleus or two sperm nuclei) were completely engorged with reserves and released from their microsporangia. The endothecium and connective cells were maximally thickened as indicated by the appearance of fibrous bands (Fb), and the anther began to desiccate, causing the anther to open up (as indicated by an arrow in Fig. 1m). In contrast, microspore development in the sterile plants was strikingly impaired. Since the tapetal cells developed large vacuoles at the tetrad stage, they continued to swell with expanded vacuoles and filled the center of the locus where the tetrads

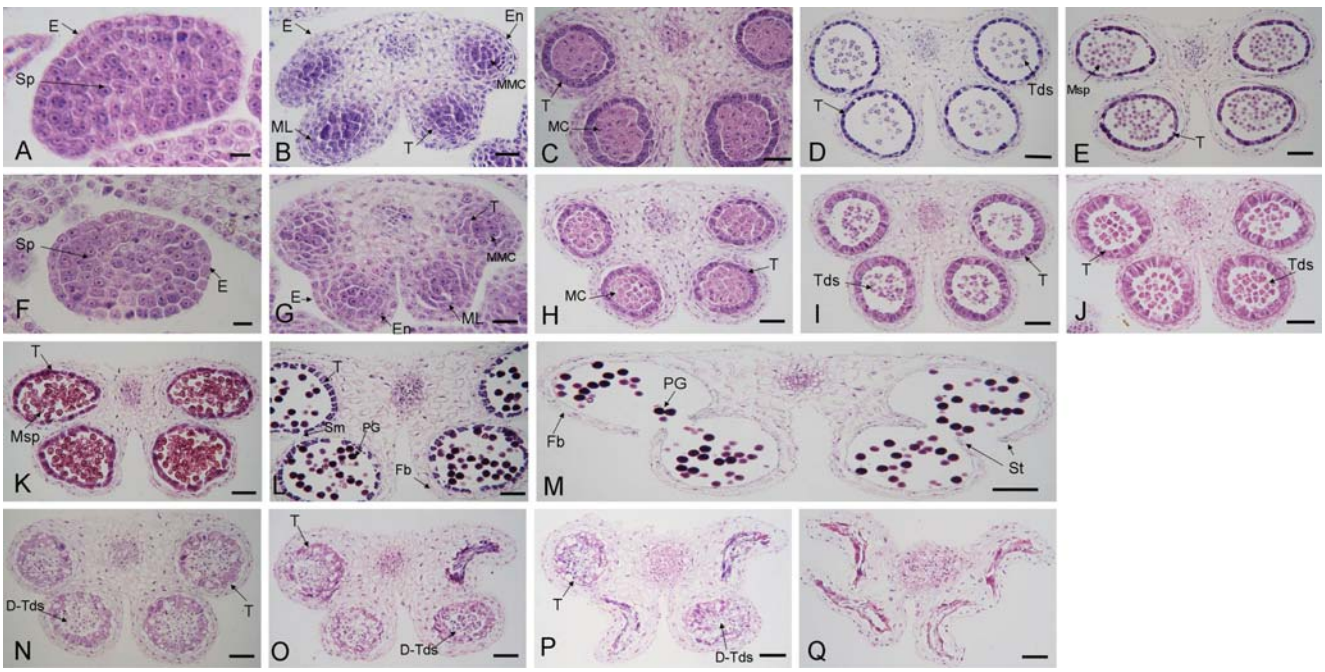

Fig. 1 Comparative study of major events during *B. napus* anther development. Flowers were fixed and embedded in white resin and sliced into 6 µm transverse sections as described in the "Material and Methods" section. The flower sections were stained in hematoxylin and anthers were photographed by bright-field microscopy. *E* epidermis, *SP* sporogenous cells, *En* endothecium, *MMC* microspore mother cells, *ML* middle layer, *T* tapetum, *MC* meiotic cell, *Tds* tetrads, *Msp* microspores, *Sm* septum, *PG* pollen grain, *Fb* fibrous bands, *St* stomium, *D-Tds* degenerated tetrads. Scale bars denote 100 µm in **m** and 50 µm all others. Fertile (**a**–**e**, **k**–**m**) and sterile (**f**–**j**, **n**–**q**) showing (1) sporogenous mass stage (**a** and **f**), (2) premeiosis stage (**b** and **g**), (3) meiocyte stage (**c** and **h**), (4) tetrad stage (**d** and **i**), (5) early microspore stage (**e** and **j**), (6) vacuolated microspore stage (**k**, **n**–**q**), (7) bicellular pollen stage (**l**), (8) late or engorged pollen stage (**m**)

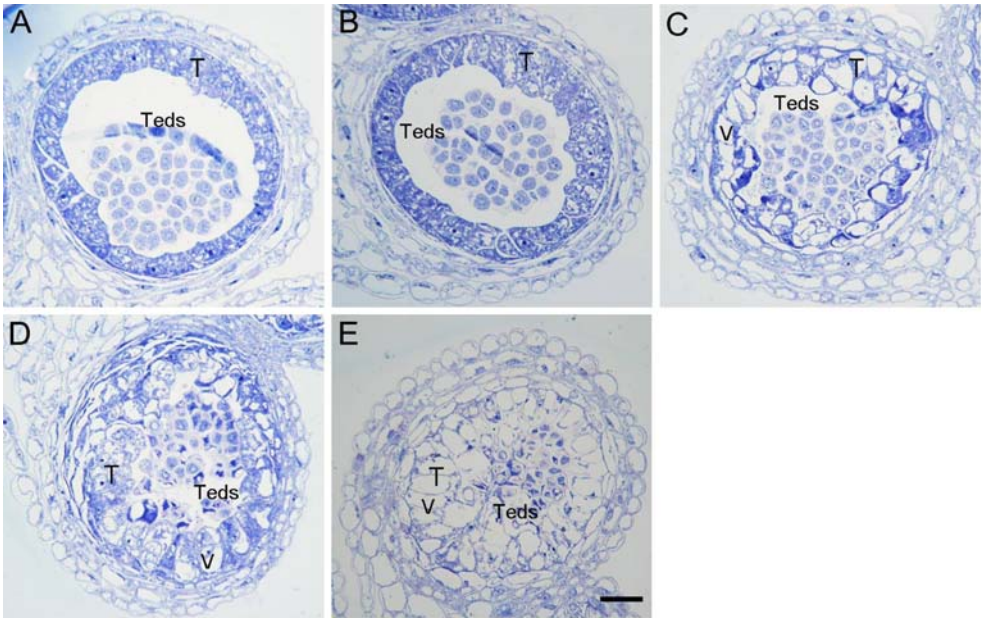

Fig. 2 Bright-field photographs of anther development in fertile and sterile plants. Stamens were fixed, embedded, and sliced into 1 μm transverse sections as described in the "Material and Methods" section. The sections were stained in toluidine blue and anther locules were examined by microscopy. **a**, **b** Fertile anther locules; **c**–**e** sterile anther locules. Tapetal cells were swollen and had excess vacuolization (**c**).Vacuolar expansion continued in the tapetal cells and tetrads encased in a thick callose wall degenerated (**d**–**e**). *T* tapetal cell, *Teds* tetrads, *V* vacuole. Scale bars=50 μm

had collapsed and degraded. The four anther locules in sterile plants sequentially shrunk and became four crescents at the end of development (Figs. 1j, n–q and 2c–e; Table 1).

Callose Staining of Sterile Anthers

In order to determine the callose deposition pattern in sterile anthers, we examined intact tetrads isolated from anthers at the tetrad stage as well as cross-sections of anthers from meiotic to postmeiotic stages. A large percentage of tetrads enclosed in thick callose walls were found to be deformed or burst (Fig. 3a and c). Moreover, it appeared that tapetal cells in sterile anthers exhibited pronounced vacuolization and cell enlargement. When the extremely expanded tapetal cells almost occupied the whole locule of sterile anthers, callose staining

Table 1 Major cytological features of developing anthers between both genotypes (fertile and sterile)

Stage	Fertile	Sterile
Sporogenous mass Premeiosis	Archesporial cells divided to form primary parietal cells that differentiated into the endothecium, middle layer and tapetum, and primary sporogenous cells differentiated into the microsporocytes. Up to the MMC stage, there was no obvious differences in anther cellular morphology including epidermis, endothecium, middle layer, tapetum and microsporocytes found in either fertile and sterile anthers	
Meiocyte	Microsporocytes seemed normal and could undergo meiosis	
Tetrad	MMC underwent meiosis within each of the four locules and generated tetrads of haploid microspores	The majority of the tetrads of haploid microspores encased with thick callose initiated degeneration, a minority of the tetrads could release the microspores. The cytoplasm of tapetal cells was vacuolated compared with the agglomerate fertile tapetum
Early microspore Vacuolated microspore	Microspores were released from tetrads and became vacuolated. The tapetal cells had deeply stained cytoplasm but no longer had large vacuoles	The tapetal cells developed large vacuoles at the tetrad stage, they continued to swell with expanded vacuoles and filled the center of the locus where the tetrads had collapsed and degraded. The four anther locules sequentially shrunk and became four crescents
Bicellular pollen	When each vacuolated microspore began to generate an exine wall and enter mitosis, the tapetum initiated degeneration	The development of the whole anther came to an end
Late or engorged pollen	The pollen grains (microgametophytes) consisted of two or three cells (one containing the tube nucleus; the others containing the generative nucleus or two sperm nuclei), were completely engorged with reserves and released from their microsporangia. The endothecium and connective cells were maximally thickened as indicated by the appearance of Fb, and the anther began to desiccate, causing the anther to open up	

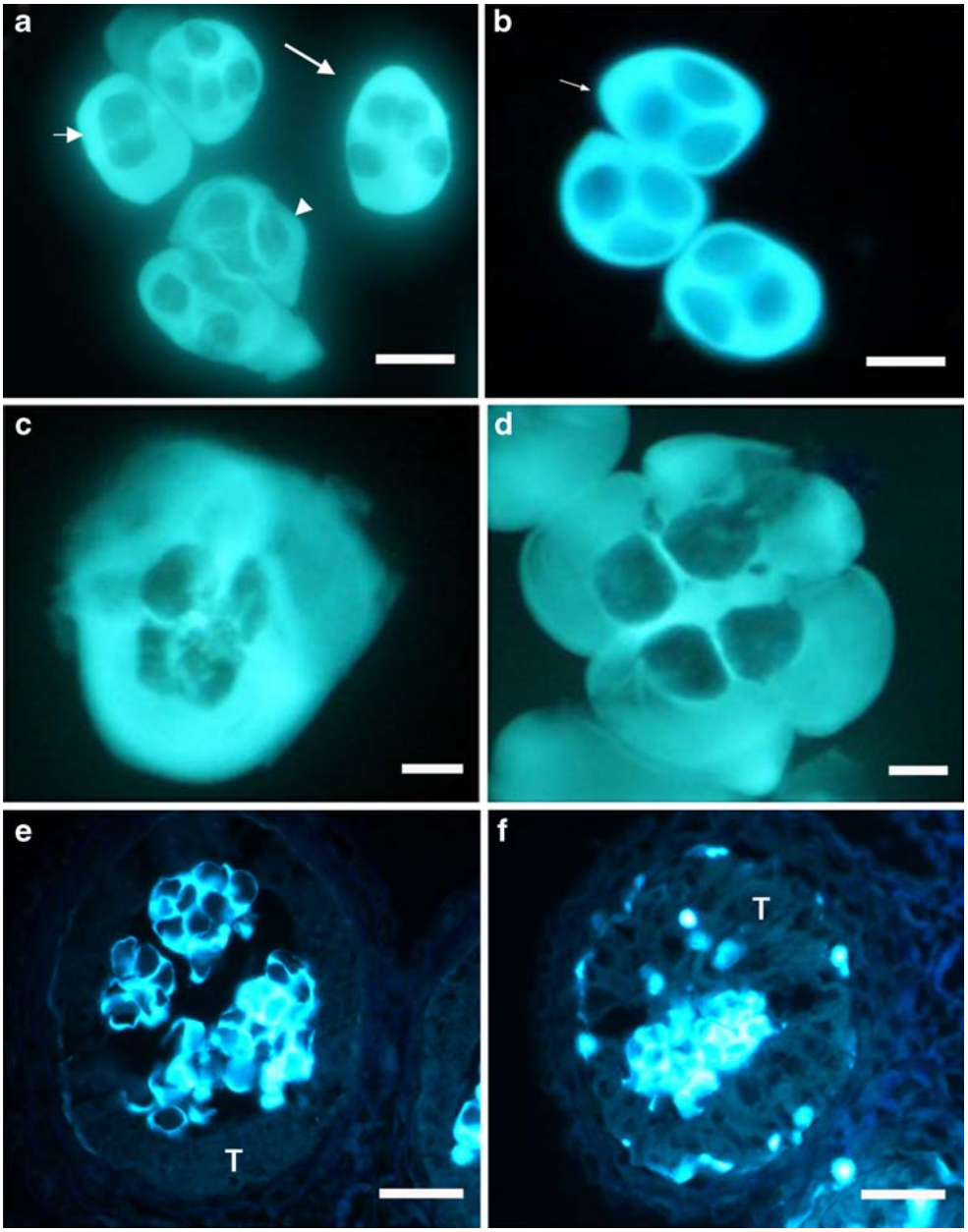

Fig. 3 Callose deposition in tetrads and released microspores of sterile and fertile anthers. **a**, **b** Aniline staining of tetrads squeezed from sterile and fertile anthers at the postmeiotic stage. **a** Microsporocyte underwent meiosis to form the dyad (*short arrow*). The majority of tetrads initiated shrinkage (*arrowhead*). A minority of microspores continued to develop, but still were packaged in thick callose wall (*long arrow*). **b** The normal tetrads were enclosed in a thick callose wall (*thin white arrow*). **c** Tetrad in the sterile anther surrounding by the callose wall degenerated. **d** Normal tetrads encased in callose wall. **a**, **b** Scale bar=20μm; **c**, **d** scale bars =50μm. **e**, **f** Aniline blue staining of cross-sections of sterile anthers at postmeiotic and tetrad stages. *T* degenerated tapetum. Scale bars=10μm

was still observed in the tetrads. Additionally, the outer tangential face of the tapetum was stained with aniline blue, but callose deposition was nearly absent in the inner tangential face (Fig. 3e and f), whereas the tetrads in fertile anthers normally developed and the microspores clustered by a callose wall (Fig. 3b and d).

EM Observations of Sterile Anthers from the Tetrad Stage to the Released Microspores Stage

We characterized the stamens of fertile and sterile plants by SEM to identify ultrastructural differences in anther morphology. Following the tetrads stage, the individual microspores were freed in the fertile anther (Fig. 4a). In sterile anthers, the haploid microspores were encased in a callose wall and surrounded by the crowded parietal tissues (Fig. 4b). In order to further characterize the male sterile phenotype, TEM was conducted on tapetal cells at the tetrad stage and the released microspore stage (Figs. 5 and 6). The most striking distinction between fertile and sterile anthers was the vacuoles observed in tapetal cells. In sterile anthers, we observed many aggregated and expanded vacuoles filled with a small amount of flocculent (fibrillar) material (Fig. 5c–f). In contrast, we did not record any enlarged vacuoles in tapetal cells from fertile anthers. At the end of the tetrad stage, tapetal cell protoplasts were no longer directly adjacent to the middle layer in the fertile anther. In addition, the tapetal cell walls were completely degener-

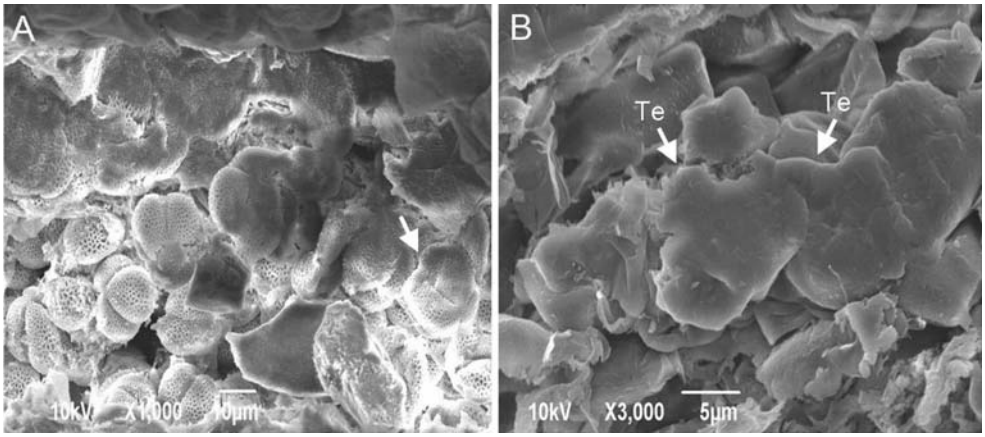

Fig. 4 Scanning electron micrographs of fertile and sterile *B. napus* anthers. **a** Microspores were released from the callose wall at the end of the tetrad stage. The microspores are somewhat angular in shape (indicated with an *arrow*). **b** The four haploid microspores produced from each microsporocyte are tetrahedrally arranged. The tetrads persistently encased with the thick callose wall were shrunken, broken, and eventually degenerated. *Te* tetrad

ated, and a large amount of fibrillar material produced by the tapetal cells was present in the locule around each cell (Fig. 5b). In contrast, tapetal cells in sterile anthers remained connected to each other by plasmodesmata. Moreover, the plasmodesmatal connections between adjacent tapetal cells were filled with the cytoplasm leaking from the vacuolated cells. Both types of tapetum derived from either fertile or sterile anthers contained groups of electron-translucent vesicles (Fig. 5a–c and e) and the nuclei were apparently located in the tapetal cell. During premeiosis II, the endoplasmic reticulum was freely distributed in the cells. After meiosis, the tapetal cells of fertile anthers were rich in stacks of endoplasmic reticulum and demonstrated signs of active mitochondria metabolism such as mitochondrial elongation and the presence of dividing organelles (Fig. 5a, b). Less dynamic mitochondria were prominent in sterile tapetal cells and the endoplasmic reticulum was loosely scattered into the tapetum (Fig. 5f). At the end of the tetrad stage, plastids were apparent in both genotypes. Those detected in sterile anthers had small electron-dense plastoglobuli (Fig. 5f) which were absent in fertile anthers. We observed less pronounced differences in the cytoplasm of fertile and sterile anthers, which were likely associated with the ellipsoidal, electron-dense structures thought to be lipid body precursors (Fig. 5a and f).

During the released microspore stage, the major difference observed between sterile and fertile anthers was the absence of tapetal transition to the secretory type, resulting in the loss of tapetal secretory function in sterile anthers. As observed in fertile tapetal cells (Fig. 6a), the cell walls of the tapetum were completely degenerated and electron-translucent vesicles were present in the cytoplasm in increased abundance than in sterile anthers (Fig. 6b). Fertile tapetal cells appeared more metabolically active than sterile tapetal cells due to the presence of abundant plastids with numerous electron-dense plastoglobuli containing an accumulation of osmiophilic material, the so-called elaioplasts. Nevertheless, tapetal cells of sterile plants intruded into the locule after losing their cell walls, while the plasmalemma was reorganized. After intrusion, the tapetal cytoplasm usually fused, but in some cases, remained intact and finally surrounded the tetrads where a small number of microspores were released from it.

In conclusion, tapetal cells in fertile anthers formed a regular layer surrounding the locules and had a spongy appearance with clusters of small vesicles at the tetrad stage, which indicated that polar secretory type cells had been formed. However, in sterile anthers, tapetal cells were abnormally vacuolated and enlarged, which resulted in an irregular layer with excessive division. Moreover, TEM analysis demonstrated that secretory tapetal cells were not present in sterile anthers, which indicated that the transition of the tapetum to the secretory type was probably aberrant.

In addition to the defects in the tapetum of sterile plants, transmission electron micrographs of cross-sections of sterile anthers were characterized in detail in terms of microsporocyte and tetrad abnormalities. Large cytoplasmic channels connected microsporocytes to each other in fertile anthers (observed in semithin sections; data not shown). Numerous small vacuoles were found throughout the microsporocytes cytoplasm. The nucleolus was centrally located, the chromatin diffused, and the nuclear membrane was intact (Fig. 7a). In contrast, within sterile microsporocytes, the nucleolus showed signs of breaking down and chromatin within the nucleus was visibly thickened (Fig. 7b). Both genotypes underwent meiosis, resulting in the formation of tetrads of haploid microspores. Tetrads derived from sterile anthers remained enveloped by the highly vacuolated tapetum, and only two or three microspores from individual tetrads were usually visible in a section (Fig. 7c–f). Individual tetrads were completely encased by a thick wall consisting of the original microsporocyte callose wall during and after cytokinesis. During the tetrad stage, within the callose wall, a microspore-produced cell wall, primexine deposition was absent in the sterile plant (Fig. 7d–j), leading to the defection of probaculae that establish the pattern of exine

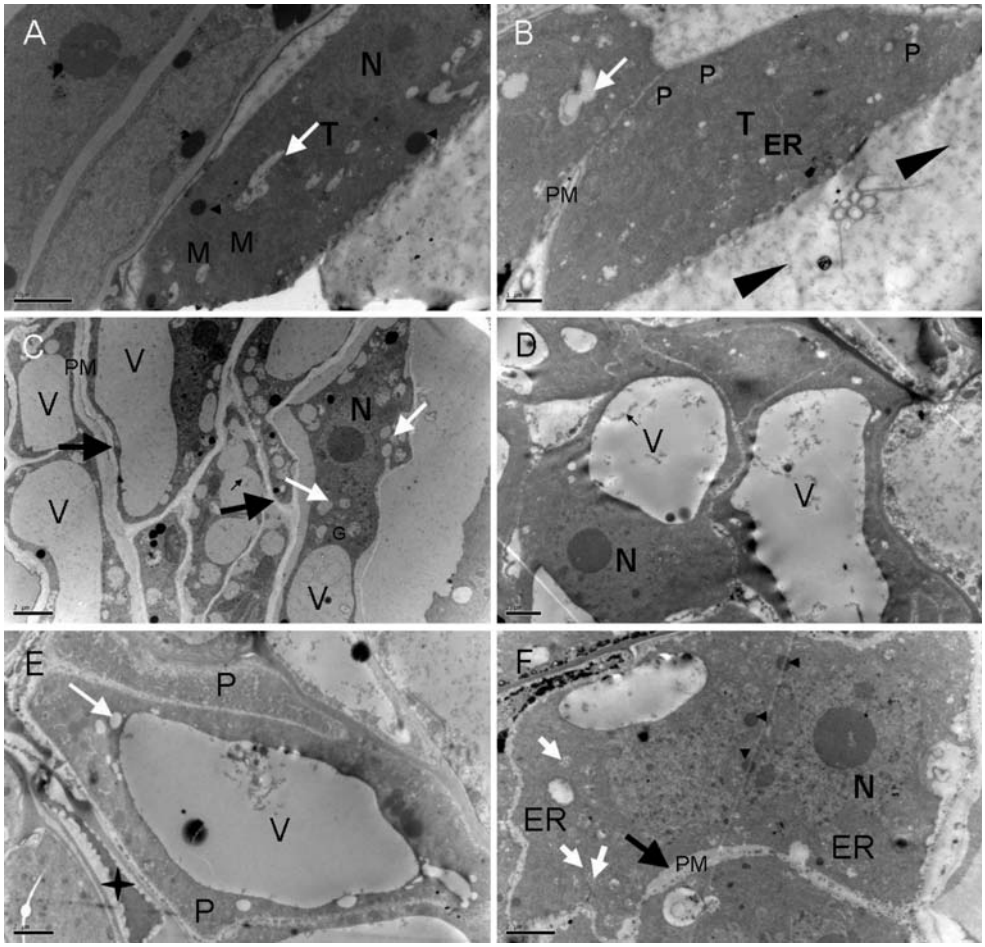

Fig. 5 Portions of the anther wall of the fertile type and the sterile type with an emphasis on the tapetum at the tetrad stage. **a**, **b** Tapetal cells in fertile anthers; **c**–**f** abnormal tapetal cells from the sterile anthers. Both types of tapetal cells contain groups of electron-translucent vesicles (*white long arrows*) and the nucleus is visible. Tapetal cells of fertile plants are rich in stacks of endoplasmic reticulum surrounding the nucleus (**b**). While less dynamic mitochondria could be observed in the sterile tapetal cells. From **c**–**e**, an abundance of vacuoles are expanding and cytoplasm is reduced in the sterile tapetal cell. Vacuoles are filled with a small amount of a flocculent (fibrillar) material indicated by the *small black arrows* in **c** and **d**. Plastids are apparent in both genotypes; those from sterile plants have small electron-dense plastoglobuli (*white short arrows* in **f**), which are absent from the fertile type. Ellipsoidal, electron-dense structures thought to be lipid body precursors are present in cytoplasm from both genotypes (*black arrowheads* in **a** and **f**). At the end of the tetrad stage, tapetal cell protoplasts are no longer directly adjacent to the middle layer in the fertile anther. In addition, the tapetal cell walls have completely degenerated and a large amount of the fibrillar material produced by the tapetal cells is present in the locule around each cell (*black thin arrowheads* in **b**). By contrast, cells of the tapetal in sterile anther remain connected to each other by plasmodesmata which have been served or were in the process of becoming so are indicated by *large arrows* in **c** and **f**. Moreover, the plasmodesmatal connections between adjacent tapetal cells are filled with the cytoplasm leaked out from the vacuolated cells (*asterisk* in **e**). *T* tapetum, *M* mitochondria, *G* Golgi bodies, *P* plastids, *N* nucleus, *ER* endoplasmic reticulum, *V* vacuole, *PM* plasma membrane. **a** and **f** Bars=2 μm, **b**–**e** bars=1 μm

wall sculpting of the mature pollen grains. In some haploid microspores arranged in tetrads (Fig. 7h), the nucleolus pressed against the nuclear membrane, which itself showed signs of breaking down. In fertile anther, the lining of the plasma membrane in each haploid microspore appeared as smooth undulations which serve as specific sites for further deposition of electrodense material (sporopollenin). However, the deposition of sporopollenin did not occur in sterile anthers due to the degenerated tapetum (Fig. 7i). Within sterile anthers, the cytoplasm of haploid microspores encased in tetrads or the free microspores released from the tetrad was filled with numerous small vesicles that become larger during later developmental stages (Fig. 7f–j).

DNA Fragmentation in Fertile and Male Sterile Anthers

The phenotypic analysis described above revealed the distinctions between the differentiation and degradation of tapetal cells and tetrads in fertile and male sterile *B. napus* anthers. In plants, the degeneration of the tapetum is considered to be the result of programmed cell death (PCD), which can be monitored by detecting cleavage of

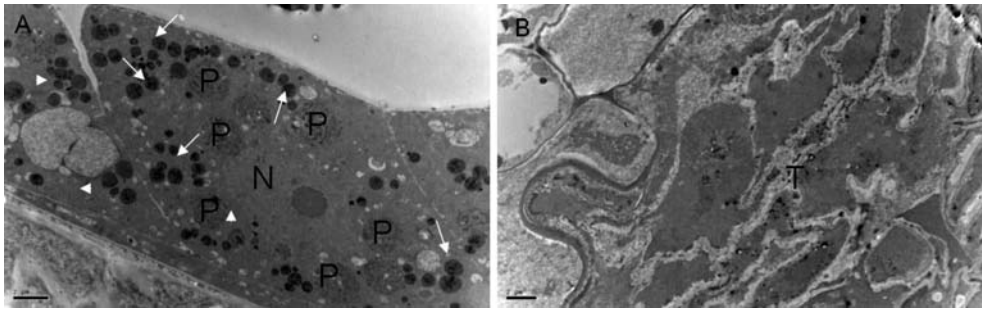

Fig. 6 Tapetal cells from fertile and sterile plants during the released microspores stage. **a** The tapetum maintains its integrity as a tissue and the cells are filled with many tapetosomes (*white arrows*) and plastids with an intense accumulation of electron-dense deposits. Nucleus is apparent in each cell. Endoplasmic reticulum (*white arrowheads*) can still be identified. *N* nucleus, *P* plastids. Scale bar= 2 μm. **b** In the sterile anther, the tapetal cells do not retain their shape, lose their cell walls, intrude into the locule, and subsequently enclose the tetrads or a few microspores. *T* tapetal cell. Scale bar=2 μm

nuclear DNA. In order to test whether sterile anthers are defective in PCD, we performed the TUNEL assay in both fertile and sterile anthers. After analysis of a range of developmental stages, TUNEL-positive cells were first detected in the tapetum and tetrads of sterile anthers at the tetrad stage (Fig. 8b). However, no fragmented DNA signals were observed in fertile anthers at the same stage (Fig. 8a). These observations demonstrated that the PCD of the tapetum commenced at the tetrad stage in the sterile anthers and that premature apoptosis was associated with male sterility in *B. napus*.

Discussion

Increase in Tapetal Vacuolar Volume Correlates with Tetrad Degeneration

In our microscopic analyses of cellular events occurring in RGMS *B. napus*, the most noticeable is permanent overexpansion of vacuoles in tapetal cells starting at the early tetrad stage. The generally recognized functions of vacuoles include storage (ions, metabolites, and proteins), digestion, pH and ion homeostasis, turgor pressure maintenance, biotic and abiotic defense responses, toxic compound sequestration, and pigmentation (De 2000). More recently, it has been suggested that this organelle plays essential roles in tropic responses, plant development, and signal transduction (Kato et al. 2002a, b; Morita et al. 2002; Surpin et al. 2003). As previously reported in the wild type of *Arabidopsis thaliana*, a drastic reduction that appeared in tapetal vacuoles occurs during the tetrad stage due to the abundant secretion of vacuolar contents. Because this vacuolar reduction coincides with the separation of tetrads through callose wall degradation, it is possible that the secreted material includes cell wall-degrading enzymes. Based on the rapidity of secretion into the locule space, these enzymes might first be stored in tapetal vacuoles and subsequently released into the locule at the appropriate time (Wu and Yang 2005).

Proteins destined for the lumen of the vacuole generally contain a signal peptide (required for default entry into the endoplasmic reticulum) and also contain either a cleavable sequence-specific propeptide (N-terminal propeptide [NTPP]; contains the core canonical sequence NPIR) or a nonsequence-specific cleavable C-terminal propeptide (Vitale and Raikhel 1999). In *Arabidopsis*, 14 β-1,3-glucanases, five polygalacturonases, and two endocellulases found to be expressed highly in young floral buds encompassing the male meiotic stage were predicted by the Target P V1.0 algorithm. A single NTPP signal following the signal peptide cleavage site was indentified in these proteins, except for the glycosyl hydrolase family protein, At4G29360, where two NTPP signals were detected (Wu and Yang 2005). The abundance of the NTPP signals in β-1,3-glucanases and polygalacturonases suggests that some of these enzymes are localized to tapetal vacuoles. In wild type *Arabidopsis* anthers at the early tetrad stage, the tapetal cells attain their maximal volume, but towards the end of the tetrad stage, they are drastically reduced in size and retain their reduced size thereafter (Izhar and Frankel 1971). This reduction in tapetal cell size mainly results from the size of their vacuoles that are the major contributor to tapetal cell volume. Following tetrad formation, exine synthesis begins in the microspore. During this process, callase (β-1,3-glucanase) is secreted by tapetal cells and released into the locular space where finally the callose wall is degraded and microspores are released (Steiglitz 1977; Steiglitz and Stern 1973). In the genic male sterile lines of *B. napus*, tapetal cells exhibited vacuolar expansion prior to tetrad separation and persistently swelled to the center of locular space, which finally lead to the degeneration of anthers. These observations indicated an absence of wall-degrading enzymes released in the locule at the appropriate time. Retarded dissolution of the callose wall affected tetrad separation and microspore development. Furthermore, the

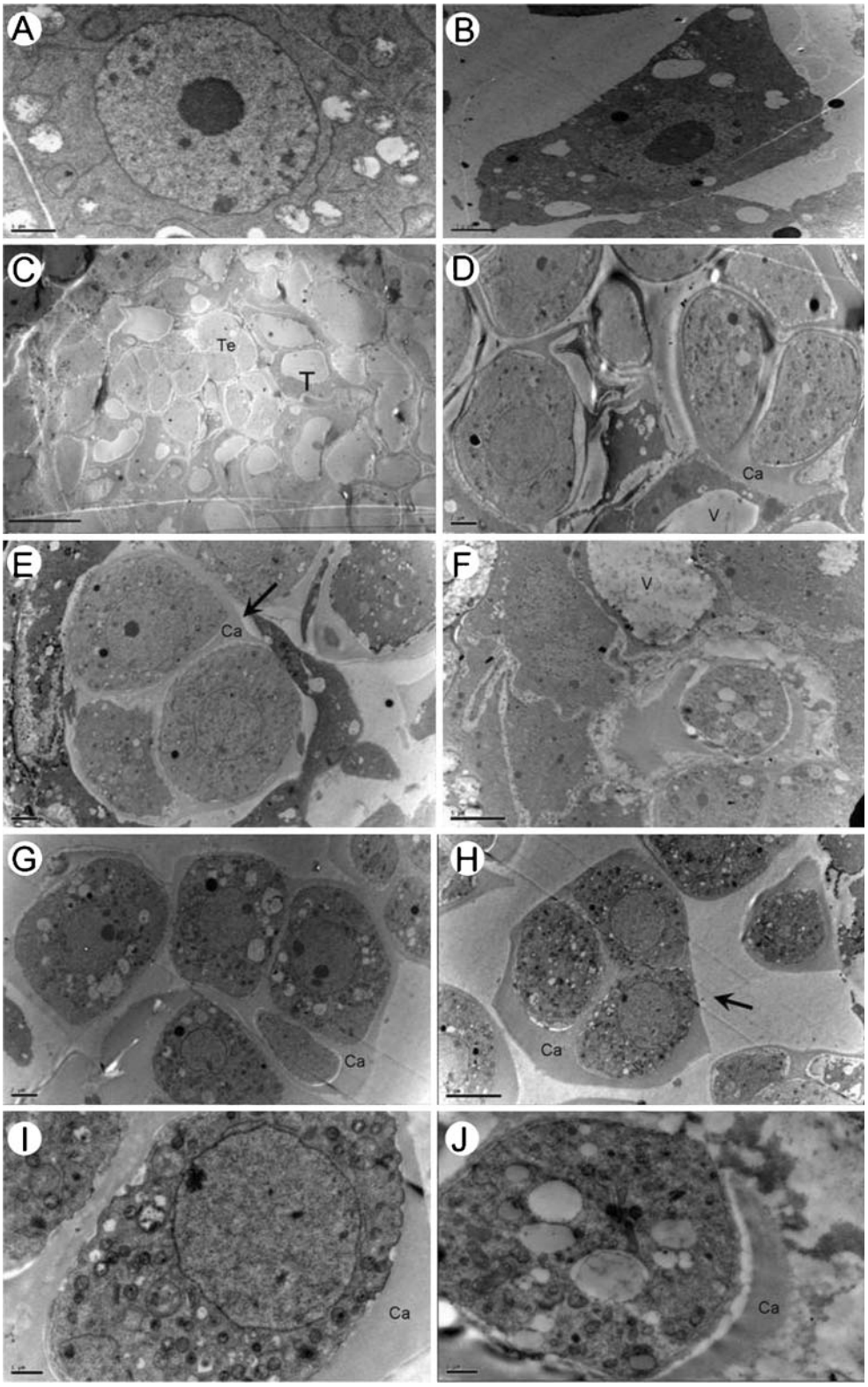

Fig. 7 Ultrastructural features of microsporocytes in the meiosis stage from fertile and sterile plants. **a**, **b** An equivalent developmental stage of meiosis in fertile and sterile anther. Bars=1 μm. **c**–**j** Transmission electron micrographs of cross-sections through anthers of sterile plants. *Ca* callose, *V* vacuole. Tetrads are indicated by *black arrows*

tetrads encased tightly in their callose walls retained their large size and gradually collapsed. Although only a few microspores enclosed with the thick callose wall were probably released from the tetrad, patches of electron-dense material rather than the developing primexine as evidenced by the uniformly shaped probaculae lined the microspore walls. We suggest that the timing of callose wall degradation is under strict regulation and is pivotal for the formation of primexine, which provides a blueprint for the exine pattern on the mature pollen grains.

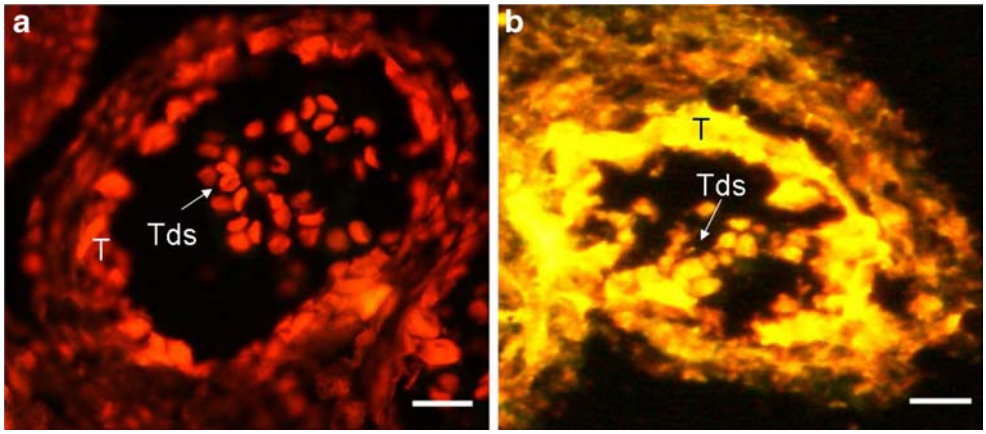

Fig. 8 DNA fragmentation in fertile and sterile anthers. Anthers in fertile and sterile types were compared at the tetrad stage using the TUNEL assay. Nuclei were stained with PI indicated by red fluorescence, while yellow fluorescence is TUNEL-positive nuclei staining. *T* tapetum. Scale bars=50 μm. **a**, **b** Fertile and sterile locules at the tetrad stage. Strong TUNEL-positive signal was detected in the tapetum and tetrads in the sterile locule, indicating that DNA fragmentation initiated at this stage

Tapetal Cell Fate in the Recessive Genic Male Sterile *Brassica napus*

Two distinct types of tapetum are found in the angiosperms: the secretory tapetum and the amoeboid tapetum. The role of these tapetal types is physiologically different. All the substances produced by the secretory tapetum reach the microspores/pollen grains via the locular fluid. In contrast, the cytoplasm in amoeboid tapeta adheres closely to the microspores. Secretory tapetum is found primarily in dicots, while the amoeboid tapetum predominates in monocots. In fertile anthers of *B. napus*, tapetal cells formed a regular layer surrounding the locules and had a spongy appearance with clusters of small vesicles, which indicated that polar secretory type cells developed. However, in male sterile anthers, the tapetal cells were abnormally vacuolated and enlarged from the tetrad stage, which resulted in an irregular layer exhibiting excessive division. Moreover, light microscopy and TEM analysis demonstrated that secretory tapetal cells were not observed in sterile anthers, which indicated that the transition of the tapetum to the secretory type was probably aberrant. In sterile anthers, tapetal cells also intruded into the locule where intimate contact with microspores was maintained. Based on the abnormal morphological evidence, we suppose that the "spermatophytic" amoeboid tapetum derived from a secretory tapetum lacking cell wall occurred in the sterile anther at the early tetrad stage due to the morphological similarity with the amoeboid tapetum of lower plants.

Recessive Genic Male Sterility is Associated with Premature PCD in Anther Tissues

We characterized the spatial and temporal occurrence of PCD in *B. napus* anther tissues by TUNEL staining during pollen development. PCD in the *B. napus* anther tissues implies that there are cells within anthers that possess particular metabolic states that enable them to respond to certain physiological signals or stimuli and to enter the process of cell death—a process apparently required for normal pollen development (Sanders et al. 2000; Wu and Cheung 2000). As the innermost of the sporophytic layers of the anther wall, the tapetum directly contacts the developing gametophytes and provides enzymes for the release of microspores from tetrads as well as nutrients for pollen development (Goldberg et al. 1993). PCD in the tapetum is characterized by the sequential elimination of cellular structures. Tapetal cell differentiation and subsequent disintegration coincides with the anther postmeiotic developmental program. During the microspore stage, PCD extends radially from the tapetum and progressively reaches the peripheral layers and was firstly triggered in the vacuolated microspores. PCD is, therefore, a progressive and active process affecting all anther tissues, but is first triggered in the tapetum, indicating that premature or delayed degradation of the tapetum is associated with male sterility (Varnier et al. 2005).

In the sterile tapetum, TUNEL signals were detected earlier in the tetrad stage than in tapetal cells of fertile anthers. This suggested that tapetal breakdown does not occur by the normal process of PCD and might be following an alternative cell death process. The abnormal swelling of the vacuole in the tapetal cells accompanied with the shrinkage observed in the cytoplasm indicated the dysfunctional tapetal cells. The signals of PCD occurred in tapetum subsequently transferred into the loculus to the tetrads and some microspores, further blocking the process of pollen development. In addition, there were fewer mitochondria present in the abnormal sterile tapetum and they exhibited ultrastructural differences including enlargement and irregular shape. In the PET1-CMS sterile

sunflower and the sterile *Arabidopsis ms1* mutant, tapetal cells were separated into delineated masses and fragmentation of DNA was observed, but the mitochondria were not completely degraded (Balk and Leaver 2001; Vizcay-Barrena and Wilson 2006). We observed similar features in RGMS tapetal cells, suggesting a breakdown process which is passive and has no need for active mitochondria. Since the genes controlling RGMS are under the way to study, we can only speculate on the roles of these genes during the tapetum development. First, these genes may participate in the establishment of tapetal cells and regulate the secretion of enzymes required for proper cell wall formation. These processes may then trigger normal tapetal PCD to facilitate the complete release of callase into the locule at the appropriate time. Alternatively, PCD may be a "ready-to-be-activated" process in the tapetal cell (Balk and Leaver 2001). In this scenario, tapetal cells fully synthesize and secrete the required metabolites, a signal triggers PCD, and the tapetum goes through an irreversible order of events that leads to cell death (Varnier et al. 2005; Vizcay-Barrena and Wilson 2006). Genes resulting in recessive male sterility may regulate tapetal development by directly regulating the inception of PCD.

Acknowledgements We thank Dr. Heather A. Owen from the Electron Microscope Laboratory, Department of Biological Sciences in University of Wisconsin for her critical review of the manuscript. This work was financed by funds from National "973" Project (no. 2007CB109006) and National "863" Project (2006AA10Z1B8 and 2009AA101105). We are grateful to Cao Jianbo for the help with the TEM and Qin Lihong for the assistance with the SEM.

References

Balk J, Leaver CJ (2001) The PET1-CMS mitochondrial mutation in sunflower is associated with premature programmed cell death and cytochrome c release. Plant Cell 13:1803–1818

Budar F, Pelletier G (2001) Male sterility in plants: occurrence, determinism, significance and use. Life Sci 324:543–550

Carter C, Pan S, Zouhar J, Avila EL, Girke T, Raikhel NV (2004) The vegetative vacuole proteome of *Arabidopsis thaliana* reveals predicted and unexpected proteins. Plant Cell 16:3285–3303

Chen F, Hu BC, Li QS (1993) Discovery & study of genic male sterility (GMS) material "9012A" in *Brassica napus* L. Acta Scientarium Naturalium Universitatis Pekinensis 19(suppl):57–61

Chen FX, Hu BC, Li C, Li QS, Chen WS, Zhang ML (1998) Genetic studies on GMS in *Brassica napus* L. Inheritance of recessive GMS line 9012A. Acta Agronomica Sinica 24:431–438

De DN (2000) Plant cell vacuoles. CSIRO, Collingwood

Dong XY, Hong ZL, Sivaramakrishnan M, Mahfouz M, Verma DPS (2005) Callose synthase (CalS5) is required for exine formation during microgametogenesis and for pollen viability in *Arabidopsis*. Plant J 42:315–328

Fei H, Sawhney VK (1999) Ms32-regulated timing of callose degradation during microsporogenesis in *Arabidopsis* is associated with the accumulation of stacked rough ER in tapetal cells. Sex Plant Reprod 12:188–193

Goldberg RB, Beals TP, Sanders PM (1993) Anther development: basic principles and practical applications. Plant Cell 5:1217–1229

He JP, Ke LP, Hong DF, Xie YZ, Wang GC, Liu PW, Yang GS (2008) Fine mapping of a recessive genic male sterility gene (*Bnms3*) in rapeseed (*Brassica napus*) with AFLP- and *Arabidopsis*-derived PCR markers. Theor Appl Genet 117:11–18

Hong Z, Delauney AJ, Verma DPS (2001) A cell-plate specific callose synthase and its interaction with phragmoplastin. Plant Cell 13:755–768

Horner HT, Palmer RG (1995) Mechanisms of genic male sterility. Crop Sci 35:1527–1535

Hou GZ, Wang H, Zhang RM (1990) Genetic study on genic male sterility (GMS) material No. 117A in *Brassica napus* L. Oil Crops of China 2:7–10

Ito T, Shinozaki K (2002) The MALE STERILITY1 gene of *Arabidopsis*, encoding a nuclear protein with a PHD-finger motif, is expressed in tapetal cells and is required for pollen maturation. Plant Cell Physiol 43:1285–1292

Izhar S, Frankel R (1971) Mechanism of the male sterility in *Petunia*: the relationship between pH, callase activity in anthers, and the breakdown of the microsporogenesis. Theor Appl Genet 41:104–108

Johns CW, Delannay X, Palmer RG (1981) Structural sterility controlled by nuclear mutations in angiosperms. Nucleus (Calcutta) 24:97–105

Jung KH, Han MJ, Lee YS, Kim YW, Hwang I, Kim MJ, Kim YK, Nahm BH, An G (2005) Rice UNDEVELOPED TAPETUM1 is a major regulator of early tapetum development. Plant Cell 17:2705–2722

Kato T, Morita MT, Fukaki H, Yamauchi Y, Uehara M, Niihama M, Tasaka M (2002a) SGR2, a phospholipase-like protein, and ZIG/SGR4, a SNARE, are involved in the shoot gravitropism of *Arabidopsis*. Plant Cell 14:33–46

Kato T, Morita MT, Tasaka M (2002b) Role of endodermal cell vacuoles in shoot gravitropism. J Plant Growth Regul 21:113–119

Kaul MLH (1988) Male sterility in higher plants. Monographs on theoretical and applied genetics 10. Springer, New York, p 10

Kawanabe T, Ariizumi T, Kawai-Yamada M, Uchimiya H, Toriyama K (2006) Abolition of the tapetum suicide program ruins microsporogenesis. Plant Cell Physiol 47:784–787

Ke LP, Sun YQ, Liu PW, Yang GS (2004) Identification of AFLP fragments linked to one recessive genic male sterility (RGMS) in rapeseed (*Brassica napus* L.) and conversion to SCAR markers for marker-aided selection. Euphytica 138:1–6

Knapp SJ, Cox TS (1988) S1 family recurrent selection in autogamous crops based on dominant genetic male-sterility. Crop Sci 28:227–231

Li SL, Zhou XR, Zhou ZJ, Qian YX (1990) Inheritance of genetic male sterility (GMS) and its utilization in rape (*Brassica napus* L.). Crop Res 4:27–32

Li SL, Zhou ZJ, Zhou XR (1993) Inheritance of recessive genic male sterile line S45AB of rape (*Brassica napus* L.). Acta Agriculturae Shanghai 9:1–7

Li SL, Zhou ZJ, Zhou XR (1995) Three-line method of genetic male sterility for hybrid seed production in *Brassica napus* L. Acta Agriculturae Shanghai 11:21–26

Li N, Zhang DS, Liu HS (2006) The rice tapetum degeneration retardation gene is required for tapetum degradation and anther development. Plant Cell 18:2999–3014

Millar AA, Gubler F (2005) The *Arabidopsis* GAMYB-like genes, MYB33 and MYB65, are microRNA-regulated genes that redundantly facilitate anther development. Plant Cell 17:705–721

Morita MT, Kato T, Nagafusa K, Saito C, Ueda T, Nakano A, Tasaka M (2002) Involvement of the vacuoles of the endodermis in the early process of shoot gravitropism in *Arabidopsis*. Plant Cell 14:47–56

Owen HA, Makaroff CA (1995) Ultrastructure of microsporogenesis and microgametogenesis in *Arabidopsis thaliana* (L.) Heynh. ecotype Wassilewskija (Brassicaceae). Protoplasma 185:7–21

Pacini E, Franchi GG, Hesse M (1985) The tapetum: its form, function and possible phylogeny in Embryophyta. Plant Syst Evol 149:155–185

Rhee SY, Somerville CR (1998) Tetrad pollen formation in *Quartet* mutants of *Arabidopsis thaliana* is associated with persistence of pectic polysaccharides of the pollen mother cell wall. Plant J 15:79–88

Sanders PM, Anhthu QB, Weterings K, McIntire KN, Hsu Y, Lee PY, Troung MT, Beals TP, Goldberg RB (1999) Anther development defects in *Arabidopsis thaliana* male-sterile mutants. Sex Plant Reprod 11:297–322

Sanders PM, Lee PY, Biegsen C, Boone JD, Beals TP, Weile EW, Goldberg RB (2000) The *Arabidopsis* delayed dehiscence1 gene encodes an enzyme in the jasmonic acid synthesis pathway. Plant Cell 12:1041–1062

Scott RJ, Spielman M, Dickinson HG (2004) Stamen structure and function. Plant Cell 16(Suppl):S46–S60

Sorensen A, Guerineau F, Canales-Holzeis C, Dickinson HG, Scott RJ (2002) A novel extinction screen in *Arabidopsis thaliana* identifies mutant plants defective in early microsporangial development. Plant J 29:581–594

Sorrells ME, Fritz SE (1982) Application of a dominant male-sterile allele to the improvement of self-pollinated crops. Crop Sci 22:1033–1035

Steiglitz H (1977) Role of b-1,3-glucanase in postmeiotic microspore release. Dev Biol 57:87–97

Steiglitz H, Stern H (1973) Regulation of b-1,3-glucanase activity in developing anthers of *Lilium*. Dev Biol 34:169–173

Surpin M, Zheng H, Morita MT, Saito C, Avila E, Blakeslee JJ, Bandyopadhyay A, Kovaleva V, Carter D, Murphy A, Tasaka M, Raikhel N (2003) The VTI family of SNARE proteins is necessary for plant viability and mediates different protein transport pathways. Plant Cell 15:2885–2899

Tu JX, Fu TD, Zheng YL (1997) Analysis on inheritance and isolocus of the rapeseed GMS 90-2441A (*B. napus* L.). Journal of Huazhong Agricultural University 16:255–258

Varnier AL, Mazeyrat-Gourbeyre F, Sangwan RS, Clément C (2005) Programmed cell death progressively models the development of anther sporophytic tissues from the tapetum and is triggered in pollen grains during maturation. J Struct Biol 152:118–128

Vitale A, Raikhel NV (1999) What do proteins need to reach different vacuoles? Trends Plant Sci 4:149–155

Vizcay-Barrena G, Wilson Z (2006) Altered tapetal PCD and pollen wall development in the *Arabidopsis* ms1 mutant. J Exp Bot 57:2709–2717

Wang TW, Balsamo RA, Ratnayake C, Platt KA, Ting JTL, Huang AHC (1997) Identification, subcellular localization, and developmental studies of oleosins in the anther of *Brassica napus*. Plant J 11:475–487

Wilson ZA, Morroll SM, Dawson J, Swarup R, Tighe PJ (2001) The *Arabidopsis* MALE STERILITY1 (MS1) gene is a transcriptional regulator of male gametogenesis, with homology to the PHD-finger family of transcription factors. Plant J 28:27–39

Wu HM, Cheung AY (2000) Programmed cell death in plant reproduction. Development 44:267–281

Wu H, Yang M (2005) Reduction in vacuolar volume in the tapetal cells coincides with conclusion of the tetrad stage in *Arabidopsis thaliana*. Sex Plant Reprod 18:173–178

Zhang W, Sun Y, Timofejeva L, Chen C, Grossniklaus U, Ma H (2006) Regulation of *Arabidopsis* tapetum development and function by DYSFUNCTIONAL TAPETUM1 (DYT1) encoding a putative bHLH transcription factor. Development 133:3085–3095